Polyhedral Boranes

DOI: 10.1002/anie.200605126

Alkoxy Derivatives of Dodecaborate: Discrete Nanomolecular Ions with Tunable Pseudometallic Properties**

Mark W. Lee, Omar K. Farha, M. Frederick Hawthorne, and Corwin H. Hansch*

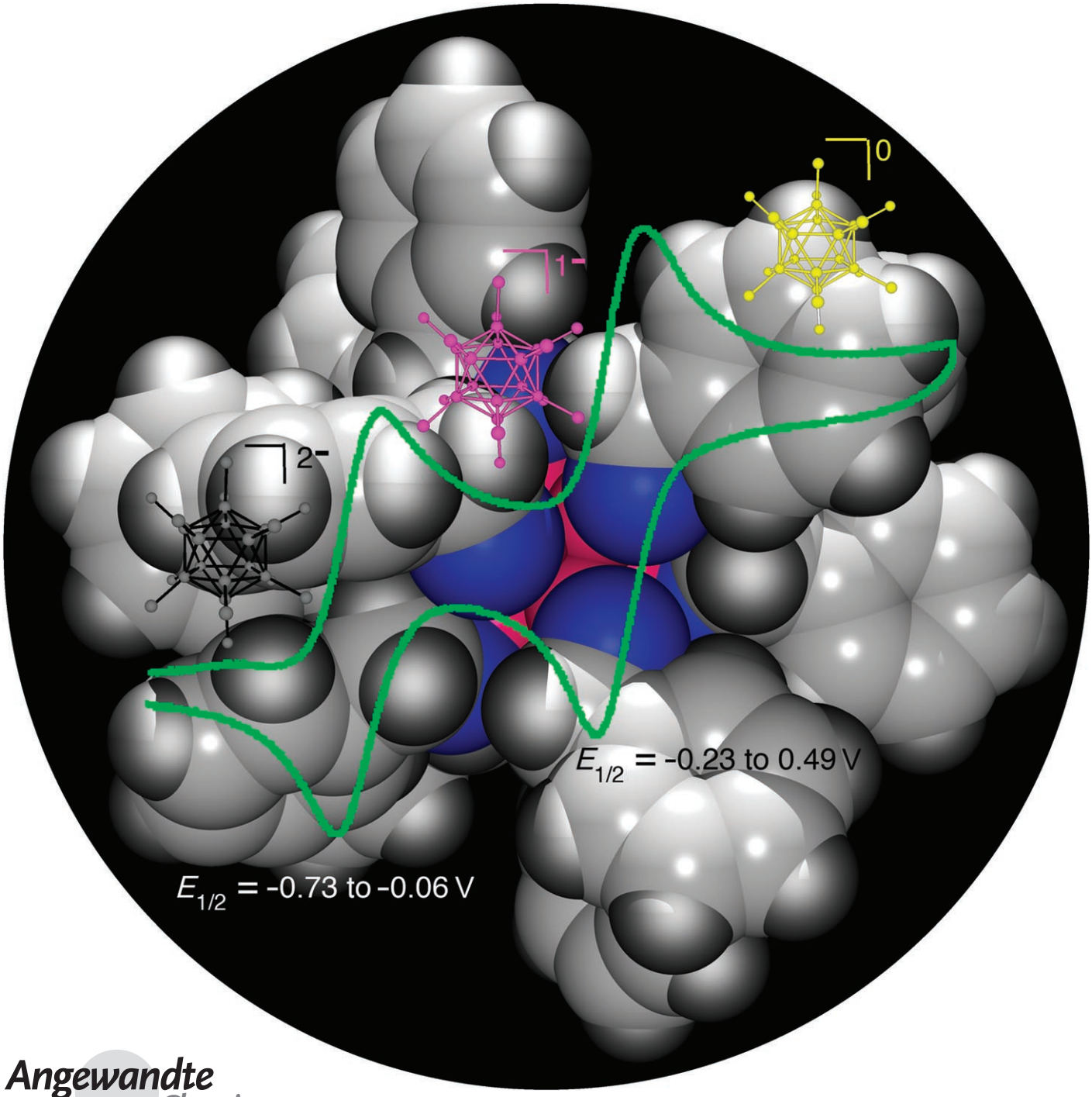

The icosahedral [*closo*-$B_{12}H_{12}$]$^{2-}$ ion exhibits extraordinary kinetic stability and is regarded as a three-dimensional aromatic species owing to extensive electron delocalization amongst its 26 cage bonding electrons.[1,2] Cage derivatization is being pursued with increasing interest,[3–7] and total substitution of all 12 B–H vertices by halogen, methyl, or hydroxy groups produces derivatives with remarkable properties.[8] Substitution with 12 hydroxy groups forms a reactive sheath which may be derivatized to form esters[9] and ethers[10] that have unique structures designated by the term "closomer".[9a,11,12]

We have previously derivatized hydroxy substituents to form the dodecabenzyl ether closomer [$B_{12}(OCH_2C_6H_5)_{12}$]$^{2-}$ (**1**).[12] It was demonstrated that this ion may be reversibly oxidized through two, one-electron processes to give the stable, *hypercloso*, 25-electron [$B_{12}(OCH_2C_6H_5)_{12}$]$^{\bullet-}$ ion and the stable, *hypercloso*, 24-electron neutral compound [$B_{12}(OCH_2C_6H_5)_{12}$] (Scheme 1).

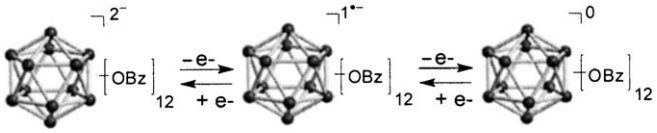

Scheme 1. Reversible oxidation of 12-benzyl closomer **1** through two one-electron oxidation steps (Bz: benzyl).

The stabilities of these *hypercloso* cages are attributed to the substituents, which supply electron density to electron-deficient cages through π back donation. This is confirmed from observations of the shortening of B–O bond lengths in the crystal structures of the 24-electron species.[12] The result is the formation of derivatives of dodecaborate that are stable in more than one oxidation state and that exhibit pseudometallic redox behavior.

Recently, we described the synthesis of a large family of ether closomers.[10] These molecules are spherical, discrete nanoparticles, which range in diameter from approximately 1 to 2.5 nm, or larger. Herein, we report the electrochemical and spectroscopic properties of these ether closomers, the structures of which are shown in Figure 1.

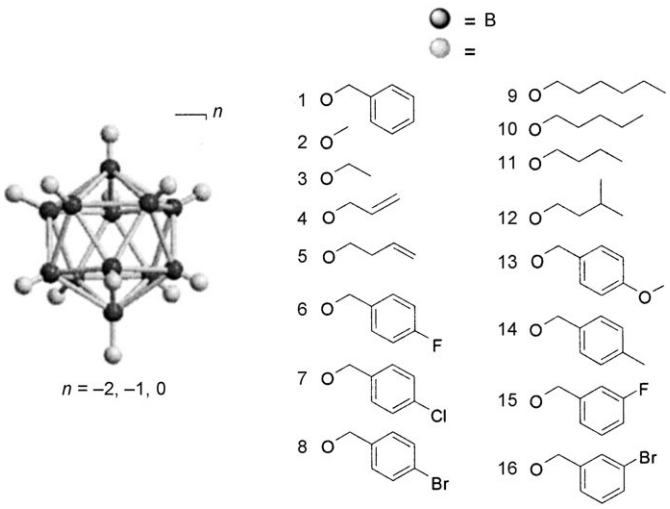

Figure 1. Structures of the ether closomers investigated electrochemically.

Cyclic voltammetry experiments with ether closomers **1**–**16** yield voltammograms with two quasi-reversible, one-electron redox couples corresponding to the [$B_{12}(OR)_{12}$]$^{2-}$/[$B_{12}(OR)_{12}$]$^{1-}$ and [$B_{12}(OR)_{12}$]$^{1-}$/[$B_{12}(OR)_{12}$]^{0} equilibria (Scheme 1). A typical voltammogram for a closomer in the presence of the ferrocene internal reference is depicted in Figure 2.

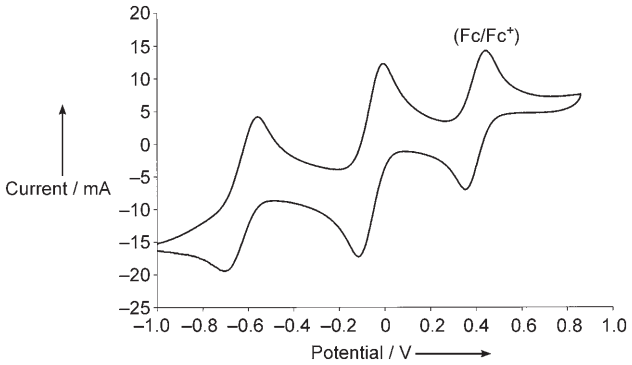

Figure 2. Cyclic voltammogram of **3** (1 mM) in 0.1 M tetrabutylammonium hexafluorophosphate in dichloromethane.

The electrochemical potentials of both redox processes are highly dependent upon the identity of the alkoxy substituents. The half-wave potentials ($E_{1/2}$) for the [$B_{12}(OR)_{12}$]$^{2-}$/[$B_{12}(OR)_{12}$]$^{1-}$ oxidation–reduction processes range from −0.73 to −0.06 V, while the values for the [$B_{12}(OR)_{12}$]$^{1-}$/[$B_{12}(OR)_{12}$]^{0} redox processes range from −0.21 to +0.49 V versus the standard hydrogen electrode (SHE; Table 1).

Excluding **2** and **13**, which undergo hydrolytic degradation, the remaining closomers were very robust in terms of chemical decomposition. Samples of **1** and **9** were unchanged following several thousand electrochemical redox cycles.

[*] Prof. Dr. M. W. Lee, O. K. Farha, Prof. Dr. M. F. Hawthorne
International Institute of Nano and Molecular Medicine
University of Missouri-Columbia
202 Schlundt Hall, Columbia, MO 65212 (USA)
Fax: (+1) 573-884-6900
E-mail: hawthornem@health.missouri.edu
Homepage: http://nanomed.missouri.edu/
Prof. Dr. C. H. Hansch
Department of Chemistry
Pomona College
645 North College Ave.
Seaver North, Claremont, CA 91711 (USA)

[**] Financial support from the National Science Foundation (NSF) (grants CHE-97300006 and CHE-0111718) and from US Borax, Inc., is gratefully acknowledged.

Table 1: Half-wave potentials [V] for closomers **1**–**16**.[a]

Closomer	Substituent	$E_{1/2}(-2/-1)$	$E_{1/2}(-1/0)$
9	1-hexyl	−0.73	−0.21
12	3-methyl-1-butyl	−0.72	−0.23
10	1-pentyl	−0.71	−0.18
11	1-butyl	−0.71	−0.18
3	ethyl	−0.63	−0.06
5	1-buten-4-yl	−0.45	−0.01
2	methyl	−0.33	0.14
4	allyl	−0.29	0.20
14	*p*-methylbenzyl	−0.45	0.09
13	*p*-methoxybenzyl	−0.42	0.15
1	benzyl	−0.29	0.22
6	*p*-fluorobenzyl	−0.21	0.37
7	*p*-chlorobenzyl	−0.11	0.47
8	*p*-bromobenzyl	−0.08	0.48
15	*m*-fluorobenzyl	−0.07	0.48
16	*m*-bromobenzyl	−0.06	0.49

[a] $E_{1/2} = (E_{pa} + E_{pc})/2$ versus $[FeCp_2]$ (Cp: cyclopentadienyl).

Sequential oxidation of the typically colorless solutions of the dianionic salts of **1**–**16** to the radical or neutral species results in the formation of intensely colored solutions. In general, solutions of the radical species are intensely red, or pink if sufficiently dilute ($\lambda_{max} = 540$ nm; $\varepsilon = 3000$–$4500\ M^{-1}cm^{-1}$), while solutions of the neutral compounds have an intense yellow color ($\lambda_{max} = 460$ nm; $\varepsilon = 7000$–$10\,000\ M^{-1}cm^{-1}$). Figure 3 presents typical electronic spectra (visible region) of a closomer in the −2, −1, and 0 oxidation states.

In addition to these absorptions in the visible region, all benzyl and substituted-benzyl closomer derivatives display unique UV absorbances attributed to these substituents.

In an attempt to further investigate the relationship between substituent properties and the electronic properties of the derived closomer, linear free-energy analyses were performed. The Hammett free-energy relationship was employed to relate substituent identity with the electrochemical properties of the closomers using Equations (1) and (2) in which σ and ρ are the Hammett substituent and reaction constants, respectively.[13]

$$\Delta G = -nF\Delta E = -2.3\,R\,T\log K \quad (1)$$

$$12\sigma\rho = \log K \quad (2)$$

Each redox potential was referenced against SHE, and $\log K$ is associated with the sequential reduction reactions shown in Equations (3) and (4).

$$^1/_2\,H_2 + [B_{12}(OR)_{12}] \rightarrow [B_{12}(OR)_{12}]^- + H^+ \quad (3)$$

$$^1/_2\,H_2 + [B_{12}(OR)_{12}]^- \rightarrow [B_{12}(OR)_{12}]^{2-} + H^+ \quad (4)$$

Table 2 lists the measured $\log K$ values associated with both reduction reactions for substituted-benzyl closomers **1**, **6**–**8**, and **13**–**16**, along with the $\log K$ values calculated using the best-fit linear equations of the data. The corresponding Hammett σ parameters are also given. Free-energy changes for each reaction were calculated using the Nernst equation at a temperature of 295 K.

Table 2: Collected Hammett substituent constants for closomers **1**, **6**–**8**, and **13**–**16** with the measured and calculated $\log K$ values associated with both reduction reactions.

Closomer	Substituent	$\log K$ (−1→−2)		$\log K$ (0→−1)		Hammett
		measured	calcd	measured	calcd	12σ
14	*p*-CH_3	−7.69	−6.62	1.54	2.83	−2.04
13	*p*-OCH_3	−7.18	−7.73	2.56	1.71	−3.24
1	*p*-H	−4.96	−4.73	3.76	4.74	0.00
6	*p*-F	−3.59	−4.07	6.32	5.41	0.72
7	*p*-Cl	−1.88	−2.18	8.04	7.32	2.76
8	*p*-Br	−1.37	−2.18	8.20	7.32	2.76
15	*m*-F	−1.20	−0.96	8.20	8.56	4.08
16	*m*-Br	−1.03	−0.41	8.37	9.12	4.68

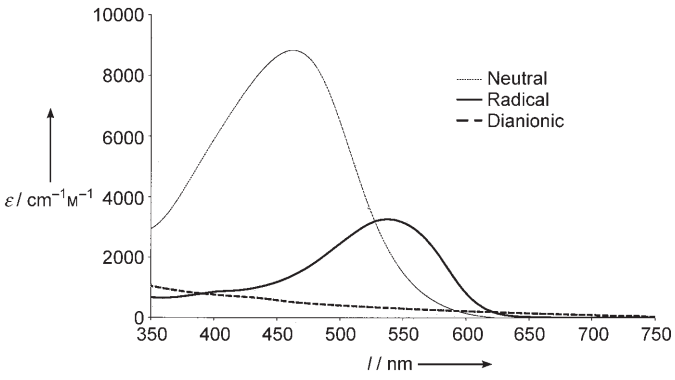

Figure 3. Visible region of absorption spectra of closomer **7** (in CH_2Cl_2) in the pseudometallic (−2, −1, 0) oxidation states.

Figure 4 shows Hammett plots of these data, and excellent correlations are obtained for both reactions with R^2 values of 0.943 and 0.890 for the −1→−2 and 0→−1 reductions, respectively. The reaction constants, ρ, for both reduction reactions are quite similar; 0.924 (−1→−2) and 0.936 (0→−1). Values of ρ near unity indicate that the sensitivity to substituent effects in these closomers is nearly equivalent to those found by Hammett for standard benzoic acid ionization. The positive ρ values are expected for both correlations and are typical for reactions in which electron density at the reaction center is increased during reaction.[13] The strong correlation between σ and free energy for the substituted-benzyl ether closomers demonstrates the large effect of substituent electronic properties on the redox potentials of the closomers.

The $E_{1/2}$ values span from −0.45 to −0.06 V versus SHE for the −1→−2 reaction and from 0.09 to 0.49 V for the 0→−1 reaction. This large range may be attributed to the cumulative effect of 12 substituents on each closomer.

In theory, the quasi-reversible oxidation of derivatives of $[B_{12}H_{12}]^{2-}$ reported herein and elsewhere[5] is possible owing

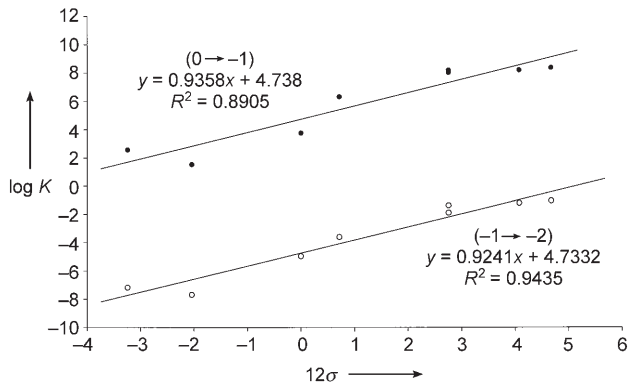

Figure 4. Plot of Hammett σ values versus free energy for the 0→−1 and −1→−2 reduction reactions of closomers **1**, **6–8**, and **13–16**.

to donation of electron density from the substituents to oxidized electron-deficient cages, accompanied by a stabilizing Jahn–Teller distortion and lowering of cage symmetry.[12] For ether closomers, this electron density is supplied by the lone electron pairs of the ether oxygen atom. Benzyl substituents with electron-withdrawing groups should decrease the electron density of the ether oxygen and therefore decrease electron donation to the boron cage. Conversely, electron-donating groups on benzyl substituents should result in increased substituent-to-cage electron donation and easier cage oxidation associated with a decreased ease of the reverse process. This is verified by the positive ρ values observed here, and the observed Hammett linear free-energy correlation matches expectations. The *m*-bromobenzyl ether closomer **16**, with $\sigma = 0.39$, has the most positive redox potentials in this series of closomers. The two benzyl substituents with negative Hammett σ constants, **13** and **14** (−0.27 and −0.17, respectively), are the two benzyl ether closomers that are more readily oxidized than unsubstituted benzyl closomer **1**. However, the relationship between alkyl and allyl closomer substituents and redox potential is more complex than the simple Hammett correlation and is seen to involve more than electronic characteristics. For example, if electronic properties were the only significant factor, the redox potentials of **2**, **3**, and **9–12** should be nearly identical. Instead, the −2→−1 oxidation of **2** requires a potential that is greater than that for **3** by 300 mV. To correlate the effects of substituents on redox potential for the non-benzyl closomers, the linear free-energy QSAR methods of Hansch were successfully employed with reactivity descriptors other than σ.[14]

Table 3 lists the changes in free energy (kcal mol^{-1}) of both reduction reactions for alkyl, alkylenyl, and benzyl closomers **1–5** and **9–12**, along with the molar refractivity (MR) and hydrophobicity (π) parameters for each substituent.[14,15] A linear regression analysis was performed between the free energy and the two parameters π and MR for both the −1→−2 and 0→−1 reduction reactions.[14] The resulting equations with the standard errors and intercept are shown in Equations (5) and (6).

$$(-1 \rightarrow -2)\ \Delta G = 9.96(1.95)\,\pi - 7.38(2.01)\mathrm{MR} + 8.41(1.94) \quad R^2 = 0.833 \tag{5}$$

$$(0 \rightarrow -1)\ \Delta G = 9.32(1.60)\,\pi - 6.89(1.65)\mathrm{MR} - 3.02(1.59) \quad R^2 = 0.867 \tag{6}$$

Figure 5 shows a plot of the measured changes in free energy versus those calculated for the −1→−2 and 0→−1 reduction reactions of closomers **1–5** and **9–12**. For both the −1→−2 and 0→−1 reactions, the correlation is strong with R^2 values of 0.833 and 0.867, respectively.

Table 3: Molar refractivity (MR) and hydrophobicity (π) substituent constants for alkyl, alkylenyl, and benzyl closomers **1–5** and **9–12** along with the measured and calculated free energies of both reduction reactions.

Closomer	Substituent	ΔG (−1→−2) [kcal mol^{-1}]		ΔG (0→−1) [kcal mol^{-1}]		MR	π
		measured	calcd	measured	calcd		
9	1-hexyl	16.83	18.56	4.84	6.52	2.89	3.16
12	3-methyl-1-butyl	16.60	15.45	5.30	3.61	2.42	2.50
10	1-pentyl	16.37	16.75	4.15	4.82	2.42	2.63
11	1-butyl	16.37	15.16	4.15	3.33	1.96	2.13
3	ethyl	14.53	10.97	1.38	−0.61	1.03	1.02
5	1-buten-4-yl	10.38	10.35	0.23	−1.17	1.91	1.61
2	methyl	7.61	9.85	−3.23	−1.66	0.56	0.56
4	allyl	6.69	8.67	−4.61	−2.76	1.45	1.10
1	benzyl	6.69	6.29	−5.07	−4.96	3.00	2.01

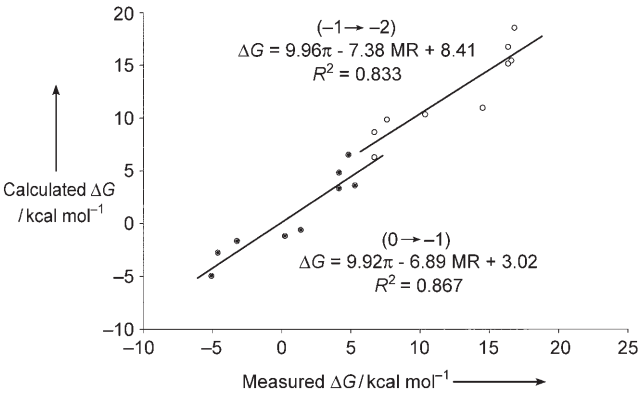

Figure 5. Plot of measured versus calculated free energies for the −1→−2 and 0→−1 reduction reactions of closomers **1–5** and **9–12**.

In conclusion, we have demonstrated the remarkable electronic properties of this family of ionic nanoparticles. Resembling metals, ether closomers are reversibly oxidized through two sequential, one-electron processes (Scheme 1). The combined range of half-wave potentials spans from −0.73 to +0.49 V versus SHE, and each redox potential is dependent upon the properties of the closomer substituents. Closomers thus exhibit donor ligand supported, metal-like redox reactions, which are accompanied by striking color

changes in accord with the three oxidation states −2, −1, and 0. Furthermore, these potentials may be predicted from Hammett and QSAR linear free-energy analysis.

This new class of polyhedral borane derivatives, with their unique properties—predictable redox potentials available through synthesis, redox-dependent spectroscopic properties, excellent chemical and hydrolytic stabilities, ease and efficiency of synthesis, and virtually unlimited structural diversity—define themselves as synthetic pseudometals that present tunable, structure-dependent redox properties. Furthermore, the relatively simple synthetic chemistry of ether closomers is amenable to their adaptation to such applications as redox-active pharmaceuticals, electrically conducting polymers, molecular devices, and the study of electrochemical phenomena associated with redox reactions of large ions of high sphericity, among others.

Experimental Section

Cyclic voltammetry was conducted using a Princeton Applied Research (PAR) model 263A potentiostat interfaced with a computer running PowerCV software. Experiments utilized a PAR microcell equipped with a Ag/AgCl reference electrode with saturated KCl solution and platinum working and auxiliary electrodes. Experiments were conducted in 0.10 M solution of tetrabutylammonium hexafluorophosphate prepared in freshly distilled dichloromethane deaerated with argon. Neutral ether closomers were used in concentrations of between 1 and 1.5 mM. The electrochemical experiments were carried out using scan rates of 50, 100, and 200 $mV\,s^{-1}$. Half-wave potentials ($E_{1/2}$) for each electrochemical reaction were calculated from the equation $E_{1/2} = (E_{pc} + E_{pa})/2$ using the cathodic and anodic peak current potentials E_{pc} and E_{pa}, respectively. Each measurement given herein is an average of four trials.

Each cyclic voltammetry experiment was conducted with and without the presence of ferrocene as an internal reference, and potentials are referenced, in turn, to the standard hydrogen electrode. For the substituted-benzyl ether closomers, which display a redox potential near that of the (Fc/Fc^+) couple, benzyl closomer **1** was used as a secondary internal reference instead of ferrocene.

Received: December 19, 2006
Published online: March 27, 2007

Keywords: boranes · cage compounds · redox chemistry · structure–activity relationships · substituent effects

[1] a) A. R. Pitochelli, M. F. Hawthorne, *J. Am. Chem. Soc.* **1960**, *82*, 3228; b) J. A. Wunderlich, W. N. Lipscomb, *J. Am. Chem. Soc.* **1960**, *82*, 4427; c) H. C. Longuet-Higgins, M. de V. Roberts, *Proc. R. Soc. London Ser. A* **1955**, *230*, 110.
[2] a) R. Hoffmann, W. N. Lipscomb, *J. Chem. Phys.* **1962**, *38*, 2179; b) M. F. Hawthorne, *Advances in Boron Chemistry*, *Vol. 82*, Royal Society of Chemistry, London, **1997**, p. 261 (Special Publication No. 201).
[3] a) W. H. Knoth, H. C. Miller, J. C. Sauer, J. H. Balthis, Y. T. Chia, E. L. Muetterties, *Inorg. Chem.* **1964**, *3*, 159; b) H. G. Srebny, W. Preetz, H. C. Marsmann, *Z. Naturforsch. B* **1984**, *39*, 189; c) O. Haeckel, W. Z. Preetz, *Z. Anorg. Allg. Chem.* **1995**, *621*, 1454.
[4] a) W. H. Knoth, J. C. Sauer, D. C. England, W. R. Hertler, E. L. Muetterties, *J. Am. Chem. Soc.* **1964**, *86*, 3973; b) T. Peymann, E. Lork, D. Gabel, *Inorg. Chem.* **1996**, *35*, 1355; c) U. Krause, W. Z. Preetz, *Z. Anorg. Allg. Chem.* **1995**, *621*, 516.
[5] T. Peymann, C. B. Knobler, M. F. Hawthorne, *J. Am. Chem. Soc.* **1999**, *121*, 5601.
[6] a) H. C. Miller, N. E. Miller, E. L. Muetterties, *Inorg. Chem.* **1964**, *3*, 1456; b) T. Peymann, E. Lork, M. Schmidt, H. Nöth, D. Gabel, *Chem. Ber.* **1997**, *130*, 795.
[7] D. Gabel, D. Moller, S. Harfst, J Rösler, H. Ketz, *Inorg. Chem.* **1993**, *32*, 2276.
[8] M. F. Hawthorne, *R. Soc. Chem.* **2000**, *253*, 197.
[9] a) A. Maderna, C. B. Knobler, M. F. Hawthorne, *Angew. Chem.* **2001**, *113*, 1709; *Angew. Chem. Int. Ed.* **2001**, *40*, 1662; b) J. Thomas, M. F. Hawthorne, *Chem. Commun.* **2001**, 1884.
[10] O. K. Farha, R. L. Julius, M. W. Lee, R. E. Huertas, C. B. Knobler, M. F. Hawthorne, *J. Am. Chem. Soc.* **2005**, *127*, 18243.
[11] M. F. Hawthorne, *Pure Appl. Chem.* **2003**, *75*, 1157.
[12] T. Peymann, C. B. Knobler, S. I. Khan, M. F. Hawthorne, *Angew. Chem.* **2001**, *113*, 1713; *Angew. Chem. Int. Ed.* **2001**, *40*, 1664.
[13] K. Wiberg, *Physical Organic Chemistry*, Wiley, New York, **1964**.
[14] For a complete discussion of the application of π and MR in QSAR analysis, see: C. H. Hansch, A. Leo, *Exploring QSAR: Fundamentals and Applications in Chemistry and Biology*, American Chemical Society, Washington, DC, **1995**.
[15] C. H. Hansch, A. Leo, *Substituent Constants For Correlation Analysis in Chemistry and Biology*, Wiley, New York, **1979**.

